EES Batteries

PAPER

View Article Online
View Journal | View Issue

Cite this: *EES Batteries*, 2026, **2**, 586

Towards an all-printed biodegradable battery

Alexis Laforgue, *[a] Asmae Mokrini,*[a] Edmond Lam,†[b] Alfred Chi Woon Leung,[b] Yali Liu,[b] Sophie Régnier,[b] Denis Rho,[b] Marie-Josée Lorrain,[b] Robert Black,[c] Andrew Wang,[c] Nathalie Chapleau,[d] Naveen Chopra,[e] Gregory McGuire[e] and Nan-Xing Hu[e]

Received 6th September 2025,
Accepted 18th November 2025

DOI: 10.1039/d5eb00164a

rsc.li/EESBatteries

During the last decades, the need for power sources has significantly intensified. Unfortunately, most of the billions of batteries produced each year end up in landfills, generating ever-increasing amounts of toxic electronic waste (e-waste). The need to develop battery technologies that are more respectful of the environment is therefore of critical importance. However, the efforts to develop such batteries are surprisingly scarce. Primary (non-rechargeable) batteries, which are being discarded after a single use, are a perfect example of a battery technology that should be replaced by a more environmentally friendly solution, to help decrease e-waste. In this study, an essentially biodegradable Zn–MnO_2 primary battery is presented, its polymeric components having been replaced by biodegradable analogues, either from existing materials or developed in-house following the principles of ecological design. Importantly, the manufacturability of each battery component has been taken into account to ensure industrial relevance. The resulting battery can be produced using high-throughput printing technologies and its performances are comparable to commercially available batteries of the same chemistry, with the added benefit of being fully degraded in a two-month period in typical composting conditions.

Broader context

Technological progress, the digitalization of society and increased consumption have led to a global increase in the production and use of electronic devices and batteries. According to recent reports, electronic waste (e-waste) is the waste stream having the highest growth rate, which poses significant environmental concerns for the years to come. The need to develop electronic and battery technologies that are more respectful of the environment is therefore of crucial importance. Single-use alkaline batteries, which largely end up in landfills, are a typical case where a replacement by an environmentally friendly solution would make sense, allowing a significant decrease of the associated corrosive e-waste. In this paper, we present the development of such a solution: a zinc-manganese primary battery containing essentially biodegradable components, that has been designed to be fabricated using high-throughput printing methods to enable low-cost industrial production. The battery exhibits equivalent performance to state-of-the-art printed batteries of the same chemistry and is entirely degraded in a two-month period under typical industrial composting conditions. This represents a significant achievement towards the development of industrially relevant sustainable battery technologies, and an important step forward towards the reduction of global e-waste.

1 Introduction

The need for power sources has significantly intensified in recent years due to the growing number of applications, including IoT (Internet of Things), consumer electronics and monitoring technologies (wearable electronics, environmental monitoring, smart packaging, *etc.*). For many applications, energy is only necessary for a limited amount of time, after which the device and its power source are discarded. The fast-growing pace of development and deployment of these new technologies is likely to significantly increase the already impressive volumes of electronic waste (e-waste). According to the 2024 Global E-waste Monitor, the total amount of e-waste was 62 million tons in 2022, nearly double the amount of e-waste generated in 2010.[1] To address this issue, a significant

[a]*National Research Council Canada, Clean Energy Innovation Research Centre, 75 de Mortagne Boulevard, Boucherville, Québec, J4B 6Y4, Canada. E-mail: alexis.laforgue@nrc.gc.ca, asmae.mokrini@nrc.gc.ca; Tel: +1-450-645-4239, +1-450-645-4181*
[b]*National Research Council Canada, Aquatic and Crop Resource Development Research Centre, 6100 Royalmount Avenue, Montreal, Québec, H4P 2R2, Canada*
[c]*National Research Council Canada, Clean Energy Innovation Research Centre, 2620 Speakman Drive, Mississauga, Ontario, L5K 1B1, Canada*
[d]*National Research Council Canada, Automotive and Surface Transportation Research Centre, 75 de Mortagne Boulevard, Boucherville, Québec, J4B 6Y4, Canada*
[e]*Xerox Research Centre of Canada, 2660 Speakman Drive, Mississauga, Ontario, L5K 2L1, Canada*
†Present affiliation: ACS Green Chemistry Institute, 1155 Sixteenth Street, NW, Washington DC 20036, USA.

effort of research has been carried out in the last two decades to develop more environmentally friendly electronic devices, the so-called "green electronics".[2,3] However, efforts for the development of more environmentally friendly batteries only started recently, the first reports appearing in the mid 2010's, mostly targeting transient power sources for edible/implantable biomedical devices.[4,5]

Early biodegradable batteries showed limited energy densities and shelf-life as well as challenging manufacturability. However, innovative concepts have emerged in the last few years. For instance, Yang *et al.* developed a paper-based battery by forming a biodegradable hydrogel within a thin paper and printing electrodes on both sides.[6] The zinc anode achieved a surprisingly high stability with cycling, enabling these batteries to be recharged multiple times with minimal performance loss, triggering the interest of a start-up, which now tries to bring the invention to the market.[7] Another example is the kirigami-inspired biodegradable battery developed by Karami-Mosammam *et al.*, based on a magnesium-molybdenum trioxide chemistry, which showed a remarkable performance, even though the manufacturability of this technology at scale is questionable.[8] Taking a more traditional approach, Lee *et al.* reported a fully biodegradable sodium-ion secondary battery, assembled with carefully selected components and displaying good performance and biodegradability.[9] Considering various scenarios of battery use, the team led by Pablo Esquivel developed several innovative concepts of biodegradable batteries, tailoring their approaches to specific applications. They first developed a primary battery based on the stacking of cellulosic and carbon papers impregnated with beeswax and using quinone-based redox active molecules, which was activated by water and could sustain a few hours of operation.[10] The same team later proposed a biodegradable battery designed for precision agriculture, inspired from the natural flow of water and nutrients in plants[11] and recently developed a cardboard-based primary battery for smart packaging applications, aimed to be recycled in the paper waste stream, even though essentially fabricated using biodegradable and non-toxic components.[12] All these technologies are indeed promising and pave the way towards more sustainable batteries. Table S1 summarizes the design, performances and manufacturability of the most advanced biodegradable batteries reported in the literature. Notably, most of these technologies have been developed at the laboratory scale, without a clear path forward for large-scale and low-cost manufacturing. Common limitations include bulky designs unsuitable to real products, long processing times for selected components (in particular polymer electrolytes such as hydrogels, usually requiring lengthy cross-linking reactions or evaporation of the processing solvent), as well as complicated device assembly methodologies, which are not easily translated into high-speed automated production. Moreover, a number of these batteries also incorporate innovative designs, such as kirigami-inspired structures to enable stretchability,[8] or novel materials, such as laser-induced graphene current collectors,[12] which can pose additional challenges in terms of manufacturability and cost.

The present work describes a biodegradable battery designed to be produced at the industrial scale using high-throughput roll-to-roll printing technologies. The concept was developed following the requirements of ecological design.[13,14] Importantly, beside being biodegradable, all battery components and degradation products need to be non-toxic to the environment and to living species. The sets of requirements for each component are listed in Table S2 and highlight the non-obvious challenges that must be overcome to develop a fully biodegradable battery. It was decided to avoid battery chemistries involving non-aqueous electrolytes, as most organic solvents present some degree of toxicity.[15] In particular, popular secondary chemistries such as Li-ion batteries also contain highly fluorinated salts and binders, which are strong poisoners to the environment.[16] Strongly alkaline or acidic electrolytes were also excluded, since their corrosive nature could present risks when leaked to the environment during battery degradation. Finally, the Leclanché chemistry was selected, based on a zinc (Zn) anode, a manganese dioxide (MnO_2) cathode and a water-based electrolyte having a close-to-neutral pH.

The cell manufacturability was taken into consideration in the design or selection of each component, to ensure that the fabrication processes were amenable to high-speed production. An all-printed fabrication strategy was chosen for its relative manufacturing simplicity, beside offering several advantages over the fabrication route of traditional coin, button or cylindrical cells: all-printed batteries can be made thin and flexible, and their form factor can be tailored to the application. Another key advantage for a biodegradable battery is their plastic-based packaging, which can be made biodegradable as well, contrarily to the solid metal casings of the more traditional form factors. Fig. 1 shows an exploded view of such a printed battery and a possible continuous roll-to-roll production process, employing methods already used in multiple industries, and expected to be low-cost and straightforward to set-up and operate.

Importantly, those batteries are only expected to degrade in certain conditions where both hydrolysis and biodegradation reactions by microorganisms can take place, such as typically found in a composting process. As such, there is no risk of premature battery degradation during typical storage or operation.

The specific developments of each biodegradable component are detailed in the following sections as well as in the SI.

2 Development of biodegradable components

2.1 Substrate

Many biodegradable materials have been considered as substrates for biodegradable devices, in the form of thin polymer films, fiber-made materials such as paper or cardboard, and even textiles.[2,5,12,17–19] In the case of a battery, a polymer thin film is the preferred choice to maintain all components in a

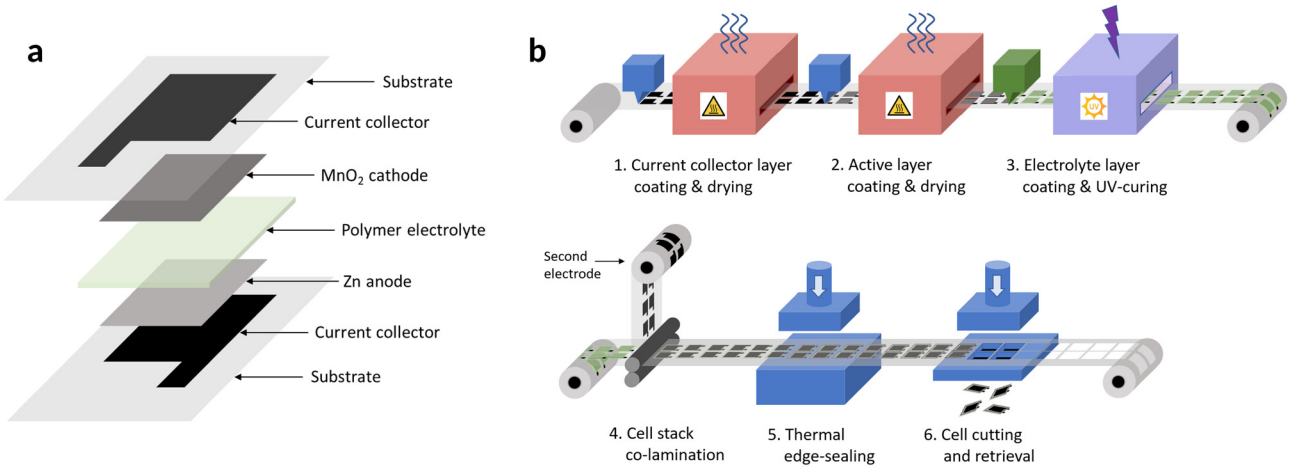

Fig. 1 (a) Schematic view of the components of a Zn–MnO_2 printed battery; (b) example of a possible high-throughput roll-to-roll process for the production of low-cost printed batteries.

closed volume (avoiding electrolyte leakage). Most biodegradable polymers are, by essence, swellable or soluble in water, which is not desirable. However, linear polyesters (biopolyesters) stand out as the only family of biodegradable polymers which do not solubilize nor swell in water.[20] Potentially suitable biopolyesters were therefore selected and tested as substrates (see SI section 2 for technical details). Even though several substrates passed the preliminary thermal stability tests (Table S3), most of them experienced deformations in the printing trials (curling, wrinkling, *etc.*), and only one type of material, PLA-D, had the necessary temperature resistance to sustain multiple printing steps without deformation (Fig. S1). PLA-D is a commercially available PLA which was extruded with a special additive (Luminy D-070) allowing to enhance the polymer crystallinity, thereby improving its temperature resistance.

2.2 Packaging

Ideally, the printing substrate would also be the battery packaging, to simplify the manufacturing process and decrease costs. However, the packaging also needs to be impervious to water vapor permeation to prevent the battery from drying out. Unfortunately, PLA is known to be permeable to water vapor, especially through its amorphous regions.[21,22] Indeed, the results show that a pouch made of thermally sealed PLA-D layers containing a paper impregnated with water lost all its water in about 10 days (Fig. S2). Developing biodegradable thin films impervious to water permeation is indeed a significant challenge. Barrier properties can be obtained either by embedding inorganic materials (ceramics or clays) into the film (composites), or by adding a metal layer to the polymer film. Composite films may appear as the best solution for a biodegradable product, in order to minimize its metallic content. However, since the inorganic additives do not form a continuous layer in composites, they only partially block the water permeation, which is not a suitable solution.[9] On the other hand, metallized PLA films (having a submicron top layer of sputtered aluminum) have been developed as humidity-controlled packaging for the food industry. These packaging solutions were tested, but their water vapor blocking properties were only marginally better than the PLA-D (Fig. S2). Therefore, an in-house solution was developed, based on the multilayer laminate design used by the pharmaceutical and Li-ion battery industries to block moisture and oxygen permeation. These multilayer laminates comprise an aluminum foil as a core layer enclosed by polymer layers (usually polypropylene as the internal thermally sealable layer and nylon as the external protective layer). An analogue of these multilayer packaging films was developed (Fig. S3). A PLA-D layer was co-extruded along with an amorphous PLA formulation serving as an adhesive tie-layer and directly co-laminated onto an aluminum foil. The multilayer laminate proved to efficiently block water permeation (Fig. S2 & S4). Further details on the development of this biodegradable multilayer laminate can be found in the SI section 2.

2.3 Electrode binders

A number of polymeric materials are traditionally used as binders in Zn–MnO_2 electrodes. Typical examples are styrene–butadiene rubber (SBR), polytetrafluoroethylene (PTFE), polyethylene oxide (PEO) or polyvinylidene fluoride (PVDF).[23,24] However, none of these polymeric binders are biodegradable. On the other hand, biodegradable polymers have also been used as battery binders (such as cellulosic materials or polyvinyl alcohol), but their water solubility usually prevents their use in aqueous batteries. Several biodegradable polymers were investigated, including poly(lactic-*co*-glycolic acid) (PLGA), chitosan, sodium alginate (SA) cellulose acetate butyrate (CAB), gelatin and agarose (Fig. S6). Although partially successful results were obtained with a number of these binders, only SA met all the required properties for both electrodes (see SI section 3 for details). SA is a water-soluble polysaccharide

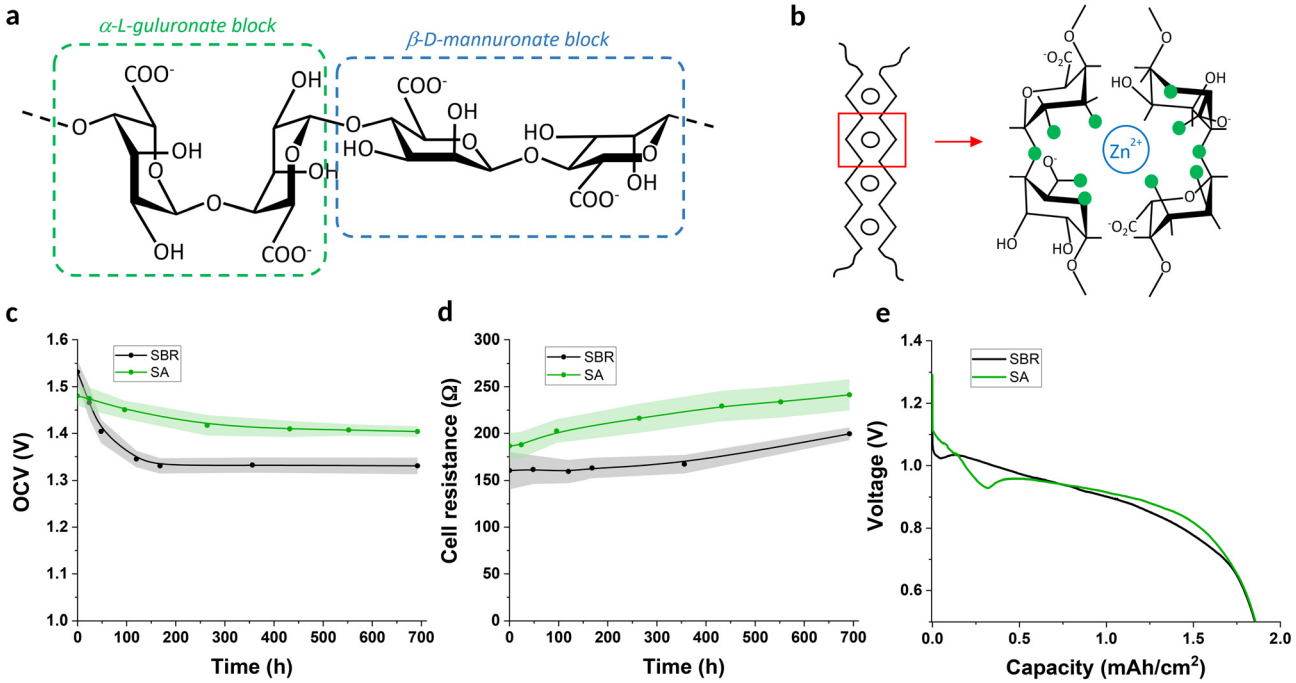

Fig. 2 (a) Structure of alginate; (b) schematic drawing of the "egg box model" as described for pairs of guluronate blocks ionically crosslinked by dications. Green disks represent the oxygen atoms involved in the coordination with the zinc ion (adapted from Braccini *et al.*)[25] open circuit voltage stability (c), cell resistance stability (d) and constant current cell discharge at 0.7 mA cm^{-2} (e) for SBR and alginate-based cells.

whose unique structure is composed of α-L-guluronate and β-D-mannuronate blocks (Fig. 2a). Interestingly, it has been shown that the presence of divalent cations such as Ca^{2+} can freeze the structure of the guluronate blocks *via* an ionic crosslinking mechanism, described as an "egg box" model (Fig. 2b), resulting in an insoluble polymer.[25] We used this concept to formulate aqueous SA-based inks that could be made insoluble in presence of the electrolyte's Zn^{2+} cations (Fig. S7). The same concept has been recently used by other researchers, confirming the promises of this ionic crosslinking concept for Zn-based battery applications.[26,27] Importantly, SA proved to prevent chelation of Zn particles and provided a remarkable particle cohesion and adhesion to the current collector layer for both Zn and MnO_2 active layers, even at contents as low as 1 wt%, which is highly desirable for the maximization of energy density as well as for large-scale production considerations. The electrochemical and resistance stability of the cell built with SA binders was relatively similar to the cell printed with traditional SBR binder (Fig. 2c and d) and reached the same discharge performance (Fig. 2e).

Biodegradable binders were also investigated for the carbon-based current collector layers. However, several issues prevented their successful use, such as insufficient electronic conductivities and inter-layer adhesion issues (see section 3–5 of the SI for details). It was therefore decided to use a non-biodegradable commercially available ink for current collector layers (Nagase Chemtex Cl-2042), based on the estimation that the binder content would be very low compared to the total mass of battery (0.05 wt%), which could be considered a reasonable compromise to deliver an essentially biodegradable battery while maintaining an optimal performance.

2.4 Gel polymer electrolyte

Multiple efforts have been reported on the development of biodegradable polymer electrolytes for sustainable batteries.[28–31] However, their processing typically requires multiple steps, including hours of solvent evaporation and/or chemical crosslinking. These excessively long processing times strongly limit the industrial adoption of such biodegradable technologies. Considering these issues, the approach taken was to integrate the product manufacturability aspect in the molecular design of the material itself, with the objective to develop a gel polymer electrolyte (GPE) that could be formulated as a printable ink and then rapidly solidified without the need for solvent evaporation or a lengthy chemical crosslinking reaction. The development was carried out in three stages, finally leading to a fully biodegradable system based on acrylated polyvinyl alcohol-*g*-polycaprolactone graft copolymer (PVA-*g*-PCL). The details of GPE developments can be found on SI section 4 and related discussions.

Fig. 3a shows the two-step synthesis reaction mechanism, yielding a rather complex polymer system, where the main chain can carry either a hydroxyl, an acetate, an acrylate function, or an acrylated PCL sidechain. It was found that an optimal balance of structural parameters had to be found to obtain the required mechanical properties. For instance, PVA-*g*-PCL copolymers have already been reported in the literature with PCL contents over 50 mol%,[32,33] but this range of highly

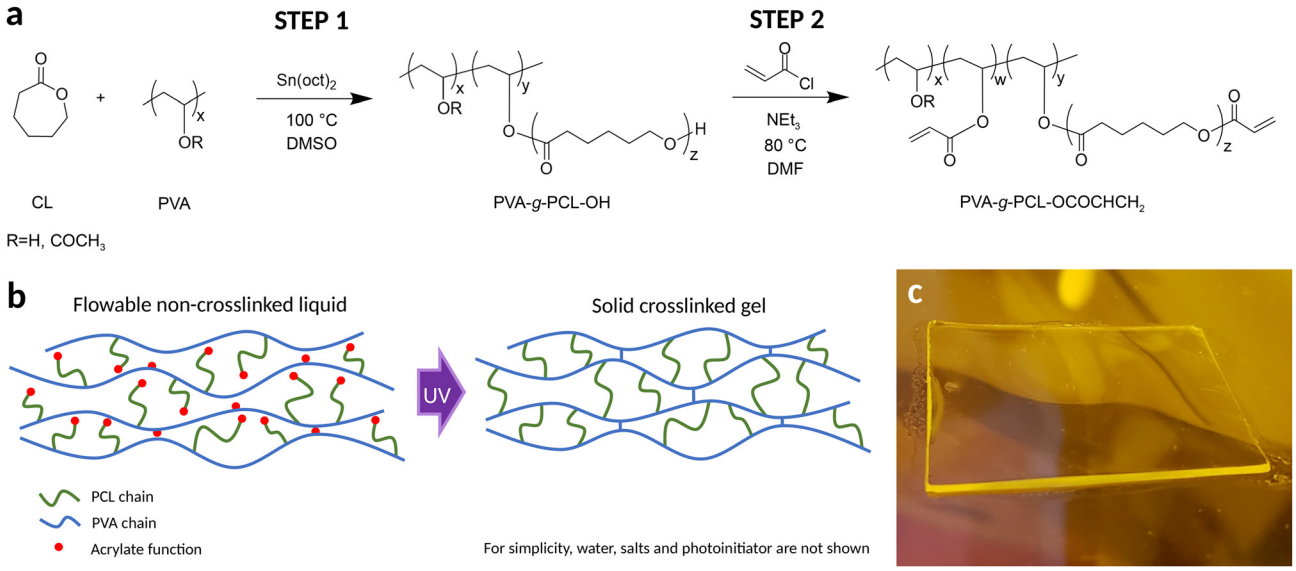

Fig. 3 GPE synthesis and formulation. (a) Two-step synthetic path of the GPE precursor macromonomer; (b) schematic rendering of the conversion of the GPE precursor solution to solid crosslinked gel using UV radiation; (c) picture of a self-standing GPE thin film after 1 s UV crosslinking.

grafted copolymers was found to yield rigid and brittle polymer gels, easily fractured upon pressure. It was determined that a range of 4 to 7 wt% of PCL provided an ideal combination of flexibility and toughness (Fig. S25 and relatied details). Following the optimization of the copolymer formulation, several aspects of the synthesis were modified and optimized for large-scale production. Key improvements included the successful replacement of the initial two-step synthesis by a one-step procedure, allowing the elimination of intermediate steps of materials precipitation, purification, recovery and drying. Also, a mixed solvent precipitation process was developed, that allowed isolation of the final copolymer without centrifugation. The combination of these improvements represented a major milestone in the development of a scalable process for the synthesis of the acrylated PVA-*g*-PCL. Scale-up was demonstrated with several batches of 400–500 g of polymers, successfully produced using a 4 L reactor (see Fig. S26 and related details).

GPE formulations were produced by simply mixing the acrylated PVA-*g*-PCL with water, electrolyte salts and LAP photoinitiator. When printed on a substrate or an electrode, then cured (for typically 1 s) using a high-power UV lamp, they yielded a solid yet flexible gel polymer electrolyte (Fig. 3b and c). The optimized GPE showed a Young's modulus of 0.15 MPa and an ionic conductivity of 60 ± 10 mS cm^{-1} (Fig. S25).

3 Manufacturing and testing

3.1 Cell printing and assembly

Batteries with the architecture shown in Fig. 1a were prepared step-by-step, following a procedure that has the potential to be further integrated into a continuous roll-to-roll process such as the one displayed in Fig. 1b. A schematic of the multi-step process is presented in Fig. S27. Fig. 4a shows final anodes on PLA-D substrate, with screen-printed current collector and Zn layers, followed by mold-printed GPE top layers. Screen-printing of the GPE layer proved to be challenging, with significant bubble formation caused by the screen itself (Fig. S29a). An alternative method based on molding was therefore developed, which allowed to print thin bubble-free GPE layers with excellent thickness control and reproducibility (Fig. S29b and c). It was found that printing the electrolyte layer on top of the Zn electrode was necessary to obtain a suitable compatibility of the electrode with the electrolyte. On the other hand, printing a GPE layer on top of the MnO_2 electrode was found unnecessary to reach optimal electrochemical performances, likely due to a sufficient wettability of the active layer with the electrolyte even after GPE crosslinking. Further details on battery fabrication can be found on section 5 of the SI.

After electrode production, battery stacks were manually assembled. A rubber roller was then used to press the layers together to achieve intimate bonding between the cell components. Thanks to its substantial mechanical properties, the GPE efficiently acted as both the electrolyte and a structural separator. The battery edges were thermally sealed using a heat sealer (MSK-130 from MTI Corporation) and then sealed within the biodegradable multilayer laminate pouch (Fig. 4b and c). Adhesive copper tape was added to the carbon tabs to enhance the electronic conductivity and the mechanical integrity of the battery poles during electrochemical testing.

The cell's characteristics and weight distribution are displayed in Fig. 4d. The cells approximate thickness and weight were 1.15 mm and 6.34 g, respectively. The total polymer content in the battery was 41.5 wt% (Fig. 4e), representing a significant part of the batteries requiring biodegradable

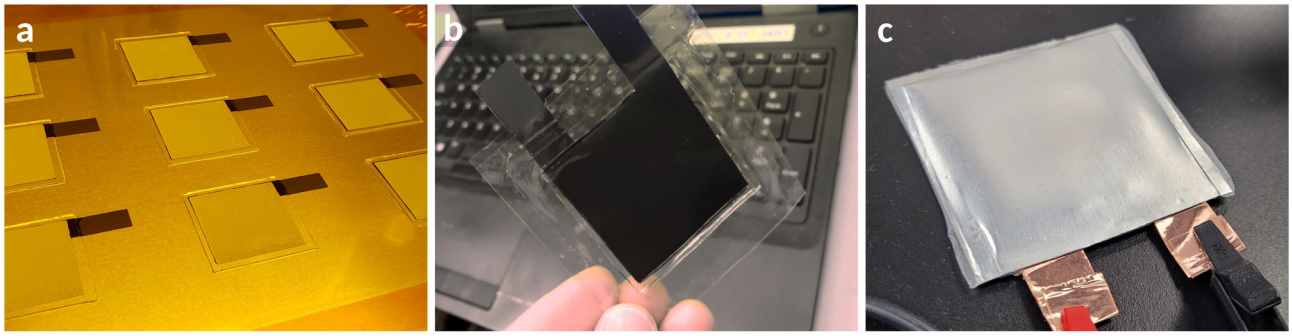

d Compostable battery characteristics

Component	Thickness (mm)	Weight (g)	Details
Substrate	0.08	0.34	PLA-D film (*x2*)
Current collectors	0.006	0.031	Nagase ChemteX CI-2042 (*x2*)
Cathode	0.04	0.394	MnO_2:Gr:SA (79:20:1) 4 x 4 cm^2
Anode	0.04	0.415	Zn:SA (99:1) 4 x 4 cm^2
Electrolyte	0.6	2,29	GPE [$ZnCl_2$:NH_4Cl] 4.5 x 4.5 cm^2
Packaging	0.15	1.21	PLA-D/Al laminate (*x2*)
TOTAL	1.15 mm	6.34 g	

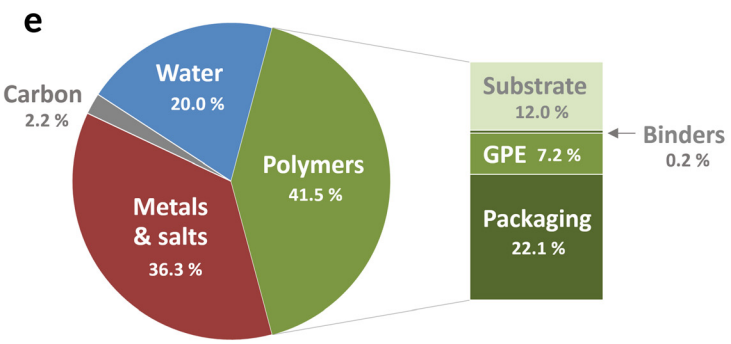

Fig. 4 (a) Mold-printed and UV-cured GPE layers on top of screen-printed carbon current collectors and Zn active layers; (b) assembled and thermally sealed battery; (c) battery thermally sealed in its compostable packaging, with copper tape reinforcement of external tabs; (d) compostable battery characteristics; (e) weight repartition of battery components.

characteristics. In these batteries, all polymers were biodegradable except the current collector binder, which represented only 0.05 wt% of the batteries (0.11 wt% of polymers). Importantly, these prototypes were a first proof of concept that might be further optimized in several aspects: anode-to-cathode capacity balance, GPE content, substrate and packaging thicknesses, *etc*. Also, the packaging layer would ideally be used as the substrate to simplify fabrication and save on materials and cost. A scenario for such an optimized cell is presented in Fig. S30, with a resulting decrease in polymer content from 41.5% to 33.3%, the majority of which being the substrate/packaging material. Hence, even in an optimized design, a third of the weight would be made of polymers that would have to be biodegradable.

3.2 Performance testing

The battery performance was assessed using standard battery testing metrics, such as open circuit voltage monitoring (OCV), electrochemical impedance spectroscopy (EIS), polarization curves and constant current discharge. The results are presented in Fig. 5 and compared to those obtained with commercially available printed cells of similar electrochemistry (Molex #133310001, Fig. S31). The OCV of the biodegradable cells showed a perfect stability at 1.38 ± 0.01 V. However, this voltage value is relatively low compared to most printed Leclanché cells commercially available (*cf.* Table S4), including the Molex cells (1.51 ± 0.01 V). The difference might be explained by the use of different active materials (in particular the type and surface state of MnO_2), differences in active layer and electrolyte formulations, as well as cell fabrication.[34,35] Indeed, the EIS Nyquist plots (Fig. 5a) show a 20% higher internal resistance for the biodegradable cell (high frequency resistance R1), suggesting a better design and electrical interconnects in the commercial cell, which can impact the OCV. The typical charge-transfers of a Leclanché cell where observed by EIS:[36] two processes related to the MnO_2 cathode and one to the Zn anode (see Fig. S32 and S33 for detailed explanations), which can be modeled using the equivalent circuit shown in Fig. 5a, each semi-circle corresponding to the impedance of a specific charge transfer. Overall, the EIS analysis showed a higher impedance for the biodegradable cell, suggesting a better power capability for the Molex cell. Polarization curves confirmed these results (Fig. 5b), the biodegradable cell demonstrating slightly slower kinetics (steeper slope) and yielding a maximum power capability of 0.19 *vs.* 0.35 mW cm^{-2} for the Molex cells. The apparent exchange current densities derived from these experiments (1.06 *vs.* 1.86 ± 0.02 mA cm^{-2}) also confirmed the lower power capabilities of the biodegradable cell (Fig. S34). This result could be due to several factors, including differences in active materials, mass loading and thickness of the electrodes, as well as thickness and ionic conductivity of the electrolyte layer. Fig. 5c shows the discharge cell profiles obtained at constant current. The biodegradable cells showed a much higher areal capacity com-

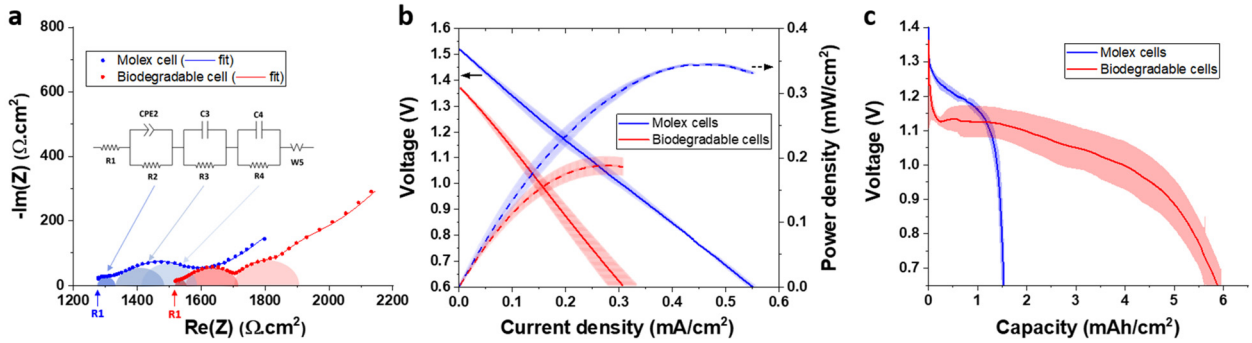

Fig. 5 (a) Nyquist plot obtained at OCV between 200 kHz and 50 mHz with 10 mV voltage amplitude; inset is the equivalent circuit used to fit the curves; R1: high frequency resistance (internal resistance); R2/CPE2: resistance and constant phase element related to a 1st MnO_2 electrochemical process; R3/C3: resistance and capacitance related to a 2nd MnO_2 electrochemical process; R4/C4: resistance and capacitance related to the Zn electrochemical process; W5: Warburg ionic diffusion resistance; (b) linear scan voltammetry at 50 mV s^{-1} between OCV and 0.6 V; (c) Galvanostatic discharge at 0.044 mA cm^{-2}. In (b) and (c), the shaded areas represent the standard deviation measured across two or three different cells.

pared to the Molex cells (5.9 *vs.* 1.5 mAh cm^{-2}), which could also explain their lower power capability. Indeed, the capacity mostly depends on the mass loading of active materials (especially the MnO_2 limiting cathode).[34] A higher loading means that the electrodes are thicker, which adds electronic and ion transport resistances, impeding the power capabilities of the cell. Interestingly, the biodegradable cells outperformed most of the printed cells currently on the market in terms of capacity (Table S4), even if it is important to stress out that cell performances are partially derived from manufacturing choices (usually tailored to specific applications), and a direct comparison can therefore be misleading. When plotted by active mass, the biodegradable cells showed an average specific capacity of 240 ± 10 mAh g^{-1} of MnO_2 (see Fig. S35), which is a typical capacity obtained from Leclanché cells (theoretical capacity of 308 mAh g^{-1}).[35,37] Overall, these electrochemical results demonstrate that the biodegradable cell performances are similar or better than the typical printed batteries of the same chemistry currently on the market.

Besides, at 6.2 mWh cm^{-2} (with a power output of 50 μW cm^{-2}), the areal energy of the battery also outperformed the most advanced biodegradable batteries reported so far, all showing energy outputs below 2 mWh cm^{-2} (*cf.* Table S1).

3.3 Compostability and eco-toxicity

Greatly distinct processes of biodegradation exist within the different ecosystems found on Earth. Ideally, multiple biodegradation conditions should be assessed before a product can be considered biodegradable.[38] In this study, the biodegradation conditions of an industrial composting facility were selected, based on the strong likelihood that most discarded single-use batteries shall be managed by such facilities. These biodegradation conditions are well defined and covered by ASTM standards. The biodegradation of the battery and its components was therefore assessed following the ASTM standard D6400 as a guideline, using the ASTM method D5338 for the testing protocol. Details on the testing methodology and results can be found in section 7 of the SI, where Fig. S36 shows a schematic representation of the testing setup. Batteries, PLA-D substrates, SA and GPE were tested along with microcrystalline cellulose powder and blank compost, as positive control and background reference, respectively. The external packaging was not included in the test nor with the batteries themselves because it was not fully developed yet. However, based on its components (PLA-D, amorphous PLA and aluminum), the compostability of its polymer components can be considered as highly probable. Yet, one disadvantage that can be foreseen is that the aluminum layer would prevent microorganisms from reaching the inside the battery. Therefore, cutting the battery before tossing it to the compost may be necessary.

Pictures of a reactor containing batteries before and after 63 days are presented in Fig. 6. It can be observed that the batteries had totally disintegrated at the end of the composting test, which suggests an efficient degradation. From the CO_2 respiration of the microorganisms, the evolution of carbon mineralization (conversion of carbon into CO_2) could be followed and the results are presented in Fig. 6c. The biodegradation of the cellulose powder reference started quickly, which was expected since it is immediately assimilable by microorganisms. SA (also a cellulosic material in powder form) followed the same trend. GPE showed a slower and more progressive biodegradation profile, which did not reach full completion within the timeframe of the composting test. GPE being based on a PVA main chain, this mineralization profile was to be expected, as already evidenced by previous studies demonstrating a relatively slow biodegradation of PVA when buried in soil.[39,40] PLA also showed limited mineralization within the timeframe of the composting test, which was also expected, since its biodegradation proceeds *via* a two-stage process starting with a long activation step, as further explained in the SI (see Fig. S41 and related discussion). These results demonstrate the compostability of all the polymeric components selected, designed and developed in this work. However, the reactors containing the batteries unexpectedly showed a limited CO_2 evolution (Fig. S42). Even if the batteries

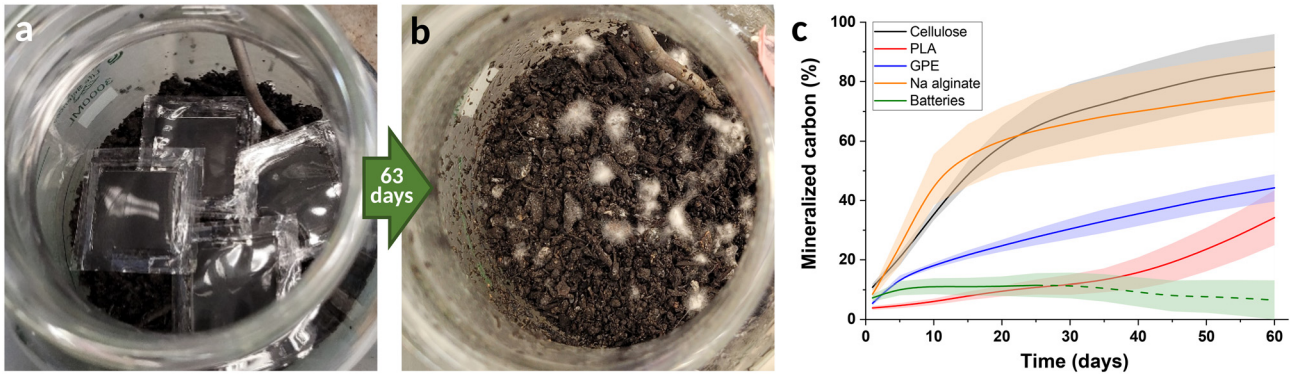

Fig. 6 Assembled batteries in a compost reactor before (a) and after (b) the composting test; (c) average mineralized carbon during the composting test, subtracted from the background reference. The shadowed areas represent the standard deviation of three reactors. The dash line part in the batteries curve shows a negative trend that is not real but demonstrates that the batteries compost released less CO_2 than the background compost during this period of time.

contain only a small amount of mineralizable carbon (11.5 wt%, Table S6), the extent of carbon conversion was very low, reaching just above 10% of the expected mineralized carbon in 25 days (Fig. 6c), after which the CO_2 release was lower than that of the background control (Fig. S42), giving an apparent negative trend on the curve. This phenomenon suggests that the compost developed some toxicity against the microbial community and inhibited its growth.

A series of complementary studies were performed. First, the eco-toxicity of the different composts was assessed using bacterial bioluminescence and rye seed germination tests (see Fig. S43 and related discussion). Both tests revealed a significant level of toxicity for the composts containing SA and batteries, with a high level of bioluminescence inhibition and no germination of seeds. The explanation for the SA compost came from its pH, clearly out of the acceptable range for plant health (9.44, Table S7). In this case, the presence of a significant amount of alginate possibly increased the alkalinity of the soil, which is known to be detrimental to plant life. Interestingly, the compost toxicity might have restrained or delayed the activity of the microorganisms, but the biotic degradation did proceed anyways, as shown in Fig. 6c. It is important to note that the alginate is present at very low content in the battery (0.2 wt% *vs.* 16.67 wt% in the compost), which did not lead to a pH increase in the battery compost (6.14, Table S7). On the other hand, very high Zn, chlorides and Mn concentrations were measured in the battery compost: 25 283 mg kg^{-1} for Zn (180 times higher than the control compost); 11 955 mg kg^{-1} for chlorides (8× higher); and 2192 mg kg^{-1} for Mn (6× higher). Even though these elements are important elements for plant life, their excess can become strongly toxic.[41,42] However, only the first two elements are believed to be the cause of the observed toxicity: Mn is only available to plants in its ionic form (Mn^{2+}), whereas the oxidized forms (MnO_x) are unavailable and therefore inoffensive.[43,44] Moreover, the compost conditions (aerobic, neutral pH) tend to stabilize the MnO_x rather than convert them to Mn^{2+}, and MnO_2 is actually used as an additive in industrial composts as a promoter of bacterial growth.[45] Since Mn is only present in oxidized forms in the battery, its presence even in important concentrations in the compost should not present any plant toxicity. On the other hand, Zn is one of the eleven heavy metals strictly regulated for compost quality, its content required to be lower than 600–2800 mg kg^{-1}, depending on the jurisdiction.[46]

Overall, this study suggests that the eco-toxicity observed in the compostability test of the battery comes from high concentrations of Zn and chlorides, and not from the materials developed. Notably, it can be speculated that in an industrial or municipal composting operation, the batteries would likely be dispersed within huge quantities of other composted materials, and that the local concentrations in Zn and chlorides should therefore not exceed the toxicity thresholds. However, this would need to be validated in the large scale operation conditions of industrial composting facilities.

These results highlight the need to develop standards better adapted to the compostability testing of multi-component devices, such as the use of more diluted conditions, *etc*. However, developing such standards was outside the scope of this work and the compostability of the batteries in more diluted conditions remains to be validated. Interestingly, a genetic study of the evolution of microbial populations clearly showed that the toxicity of the battery compost did not mean the extinction of the microbiome. Rather, a distinct biodiversity developed, more adapted to its specific environment (see section 6, 7 of the SI for a detailed analysis). Whereas the fungal populations developed in a way similar to the PLA compost, bacteria evolved in a very unique fashion, with the predominant development of bacterial families particularly resistant to high salt concentrations, some of them able to convert CO_2 into acetate or methane, which could explain the lack of CO_2 evolution (Fig. S44). This post-composting study revealed that the evolution of the biodiversity in the composts was strongly affected by the composted materials, and that the

microbiome of the battery compost was still lively and diverse, despite the presence of high quantities of Zn and chlorides, inhibiting its activity.

4 Conclusions and perspectives

A primary battery incorporating essentially biodegradable components was successfully designed and fabricated using printing techniques amenable to high-speed production. Its electrochemical performances matched or even exceeded those of typical non-biodegradable commercially available printed batteries of the same chemistry, as well as the most advanced biodegradable batteries reported so far. A key development was the design of a biodegradable gel polymer electrolyte that could be printed as a fluid layer and then converted to a solid separator *via* ultrafast UV crosslinking. This enables the potential integration of the electrolyte/separator layer printing within a high speed roll-to-roll production process flow. Further optimization and validations are still required, both in terms of component development and manufacturing process, but we consider the results of this work to be a significant step forward towards the development of industrially-relevant sustainable battery technologies able to address the growing issue of e-waste.

All developed components proved to be biodegradable and non-toxic, but the compostability study revealed an eco-toxicity of the composts containing the degradation byproducts of the whole batteries, possibly caused by the release of significant quantities of zinc and chlorides. Although this might appear as a serious challenge, the issue may actually be mitigated at the facility level by monitoring the chloride and zinc content and ensure a proper dilution of the batteries within the composted materials. Modifying the electrolyte formulation or even the battery chemistry could also be a suitable strategy to mitigate the release of potentially toxic molecules. Indeed, the biodegradable battery platform developed in this work is not limited to the Zn–MnO_2 Leclanché electrochemistry. It could also be used to design biodegradable primary and secondary batteries using other sustainable chemistries based on Mo, Mg, W, Fe, quinones, *etc.*[47,48] Even though more traditional battery chemistries such as NiMH or Li-ion batteries would present environmental risks if used with this biodegradable battery platform because of the toxicity of their intrinsic components (corrosive electrolytes, organic solvents or highly fluorinated salts), some of the components developed in this study (such as the biodegradable multilayer packaging, the UV-curable biodegradable polymer electrolyte system or the alginate binder) could be used to increase the sustainability of these batteries.[49,50]

To go one step further, the replacement of the metals and metal–oxide active materials could also be envisioned, to improve further the battery sustainability. All-polymer printed batteries have recently been developed, that replace the metal-based active materials with electroactive polymers. One example is the TAeTTOOz® battery developed by Evonik (now sold to InnovationLab).[51] By combining the biodegradable battery platform developed in this work with biodegradable active materials based on polypeptides,[52,53] lignin[54,55] or polyesters,[56] fully biodegradable and metal-free batteries could be successfully developed in a near future.

Finally, the manufacturing route that was chosen (all-printed technology) is only one example of the manufacturing methods that could be used to produce the biodegradable batteries developed in this study. Multi-electrode layered architectures could also be envisioned, using the more traditional approach of double-side coating on metallic (or carbon-based) current collectors, which is being widely used in the Li-ion industry. In this way, biodegradable batteries of higher capacities could be fabricated.

In conclusion, the results of this study show that it is possible to design environmentally friendly batteries, even though they are complex multi-component devices. In order to do so, ecological design has to be embedded in the product at its very conception and within each of its components.[9,14,57,58] Moreover, as shown by the results of the compostability and eco-toxicity studies, the physical decomposition of a multi-component device is not a sufficient criterion to assess its biodegradability, since it can release toxic chemicals into the environment. This highlights the need to develop new standards that can assess the biodegradability and environmental impacts of multi-component products in more realistic conditions.

Author contributions

Study overview, materials selection and development: AL, AM, EL, ACWL, RB, NatC, NavC, GMG, NXH; synthesis, formulations and component production: AL, EL, SR, ACWL, YL, RB, NatC, AW, NavC, GMG; cell assembly and testing: AL, RB, AW, NavC, GMG; compostability testing: AL, DR, MJL; writing of the publication: AL; revision of the publication: AL, AM, EL, RB, NavC, GMG, DR.

Conflicts of interest

The authors declare no conflict of interest.

Data availability

The data supporting this article can be found in the supplementary information (SI). Supplementary information: experimental section, additional information and discussions. See DOI: https://doi.org/10.1039/d5eb00164a.

Acknowledgements

The authors would like to thank Aymen Ghouila, Tarik Beragrag and Abdellali Ihid for their help in the production of the PLA substrates and multilayer packaging, Manon Sarrazin

and Sabine Dodard for the eco-toxicity tests, Sabahudin Hrapovic for scanning electron microscopy, as well as Miria Elias, Marie-Josée Lévesque, Christine Maynard and Julien Tremblay for the DNA sequencing and analysis. Fanny Monteil-Rivera from NRC-CEI is thanked for her useful revisions and suggestions in the writing of the manuscript. The authors thank both NRC's Clean Energy Innovation Research Center and XRCC for the funding of this work.

References

1 C. P. Baldé, R. Kuehr, T. Yamamoto, R. McDonald, E. D'Angelo, S. Althaf, G. Bel, O. Deubzer, E. Fernandez-Cubillo, V. Forti, V. Gray, S. Herat, S. Honda, G. Iattoni, D. S. Khetriwal, V. L. D. Cortemiglia, Y. Lobuntsova, I. Nnorom, N. Pralat and M. Wagner, *The Global E-Waste Monitor 2024*, United Nations Institute for Training and Research, 2024.
2 M. Baumgartner, M. E. Coppola, N. S. Sariciftci, E. D. Glowacki, S. Bauer and M. Irimia-Vladu, *Green Materials for Electronics*, Wiley-VCH Verlag GmbH & Co. KGaA., 1st edn, 2018, pp. 1–54.
3 Z. Hui, L. Zhang, G. Ren, G. Sun, H. D. Yu and W. Huang, *Adv. Mater.*, 2023, **35**, e2211202.
4 S. Yamada, *Adv. Energy Sustainability Res.*, 2023, **4**, 2300083.
5 N. Mittal, A. Ojanguren, M. Niederberger and E. Lizundia, *Adv. Sci.*, 2021, **8**, 2004814.
6 P. Yang, J. Li, S. W. Lee and H. J. Fan, *Adv. Sci.*, 2022, **9**, 2103894.
7 Flint Paper Battery website, https://www.madebyflint.co/ (accessed May 2025).
8 M. Karami-Mosammam, D. Danninger, D. Schiller and M. Kaltenbrunner, *Adv. Mater.*, 2022, **34**, 2204457.
9 M. H. Lee, J. Lee, S.-K. Jung, D. Kang, M. S. Park, G. D. Cha, K. W. Cho, J.-H. Song, S. Moon, Y. S. Yun, S. J. Kim, Y. W. Lim, D.-H. Kim and K. Kang, *Adv. Mater.*, 2021, **33**, 2004902.
10 J. P. Esquivel, P. Alday, O. A. Ibrahim, B. Fernández, E. Kjeang and N. Sabaté, *Adv. Energy Mater.*, 2017, **7**, 1700275.
11 M. Navarro-Segarra, C. Tortosa, C. Ruiz-Díez, D. Desmaële, T. Gea, R. Barrena, N. Sabaté and J. P. Esquivel, *Energy Environ. Sci.*, 2022, **15**, 2900–2915.
12 M. Navarro-Segarra, O. A. Ibrahim, I. Martin-Fernandez, C. Tortosa, J. M. Ormaetxea, M. Baumann, M. Weil and J. P. Esquivel, *Energy Environ. Sci.*, 2024, **17**, 5639–5652.
13 F. Shu-Yang, B. Freedman and R. Cote, *Environ. Rev.*, 2004, **12**, 97–112.
14 M. Navarro-Segarra and J. P. Esquivel, *Sustainable Energy Storage in the Scope of Circular Economy: Advanced Materials and Device Design*, John Wiley & Sons Ltd, 1st edn, 2023, pp. 123–143.
15 D. R. Joshi and N. Adhikari, *J. Pharm. Res. Int.*, 2019, **28**, 1–18.
16 A. Ghosh, K. Mukherjee, S. K. Ghosh and B. Saha, *Res. Chem. Intermed.*, 2013, **39**, 2881–2915.
17 C. J. Bettinger, *Trends Biotechnol.*, 2015, **33**, 575–585.
18 A. Poulin, X. Aeby and G. Nyström, *Sci. Rep.*, 2022, **12**, 11919.
19 V. R. Feig, H. Tran and Z. Bao, *ACS Cent. Sci.*, 2018, **4**, 337–348.
20 R. A. Gross and B. Kalra, *Science*, 2002, **297**, 803–807.
21 R. A. Auras, B. Harte, S. Selke and R. Hernandez, *J. Plast. Film Sheeting*, 2003, **19**, 123–135.
22 F. Wu, M. Misra and A. K. Mohanty, *Prog. Polym. Sci.*, 2021, **117**, 101395.
23 Z. Wang, R. Winslow, D. Madan, P. K. Wright, J. W. Evans, M. Keif and X. Rong, *J. Power Sources*, 2014, **268**, 246–254.
24 K.-H. Choi, D. B. Ahn and S.-Y. Lee, *ACS Energy Lett.*, 2018, **3**, 220–236.
25 I. Braccini and S. Pérez, *Biomacromolecules*, 2001, **2**, 1089–1096.
26 Y. Ding, X. Zhong, C. Yuan, L. Duan, L. Zhang, Z. Wang, C. Wang and F. Shi, *ACS Appl. Mater. Interfaces*, 2021, **13**, 20681–20688.
27 D. Xie, J. Zhao, Q. Jiang, H. Wang, H. Huang, P. Rao and J. Mao, *ChemPhysChem*, 2022, **23**, e202200106.
28 K. Wang, X. Zhang, C. Li, X. Sun, Q. Meng, Y. Ma and Z. Wei, *Adv. Mater.*, 2015, **27**, 7451–7457.
29 P. Huo, S. Ni, P. Hou, Z. Xun, Y. Liu and J. Gu, *Polymers*, 2019, **11**, 863.
30 M. Wu, Y. Zhang, L. Xu, C. Yang, M. Hong, M. Cui, B. C. Clifford, S. He, S. Jing, Y. Yao and L. Hu, *Matter*, 2022, **5**, 3402–3416.
31 N. Mittal, A. Ojanguren, D. Kundu, E. Lizundia and M. Niederberger, *Small*, 2023, **19**, 2206249.
32 K. Aoi, H. Aoi and M. Okada, *Macromol. Chem. Phys.*, 2002, **203**, 1018–1028.
33 N. Guerrouani, A. Mas and F. Schué, *J. Appl. Polym. Sci.*, 2009, **113**, 1188–1197.
34 K. Kordesch and W. Taucher-Mautner, *Encyclopedia of Electrochemical Power Sources*, Elsevier, Amsterdam, 2009, pp. 784–795.
35 N. Wang, H. Wan, J. Duan, X. Wang, L. Tao, J. Zhang and H. Wang, *Mater. Today Adv.*, 2021, **11**, 100149.
36 R. J. Brodd and H. J. DeWane, *J. Electrochem. Soc.*, 1963, **110**, 1091.
37 S. Cui, D. Zhang and Y. Gan, *J. Power Sources*, 2023, **579**, 233293.
38 A. Samir, F. H. Ashour, A. A. A. Hakim and M. Bassyouni, *npj Mater. Degrad.*, 2022, **6**, 68.
39 E. Chiellini, A. Corti and R. Solaro, *Polym. Degrad. Stab.*, 1999, **64**, 305–312.
40 A. Takasu, K. Aoi, M. Tsuchiya and M. Okada, *J. Appl. Polym. Sci.*, 1999, **73**, 1171–1179.
41 S. Hussain, M. Khan, T. M. M. Sheikh, M. Z. Mumtaz, T. A. Chohan, S. Shamim and Y. Liu, *Front. Microbiol.*, 2022, **13**, 900740.
42 C.-M. Geilfus, *Plant Cell Physiol.*, 2018, **59**, 877–886.

43 R. Millaleo, M. Reyes-Díaz, A. G. Ivanov, M. L. Mora and M. Alberdi, *J. Soil Sci. Plant Nutr.*, 2010, **10**(4), 476–494.
44 S. Alejandro, S. Höller, B. Meier and E. Peiter, *Front. Plant Sci.*, 2020, **11**, 300.
45 F. Pei, X. Cao, Y. Sun, J. Kang, Y. Ren and J. Ge, *Bioresour. Technol.*, 2023, **373**, 128708.
46 R. Stehouwer, L. Cooperband, R. Rynk, J. Biala, J. Bonhotal, S. Antler, T. Lewandowski and H. Nichols, *The Composting Handbook*, Academic Press, 2022, pp. 737–775.
47 Q. Zhao, W. Huang, Z. Luo, L. Liu, Y. Lu, Y. Li, L. Li, J. Hu, H. Ma and J. Chen, *Sci. Adv.*, 2018, **4**, eaao1761.
48 N. Hassanzadeh and T. G. Langdon, *J. Mater. Sci.*, 2023, **58**, 13721–13743.
49 S. Dühnen, J. Betz, M. Kolek, R. Schmuch, M. Winter and T. Placke, *Small Methods*, 2020, 2000039.
50 Y. Ding, X. Zhong, C. Yuan, L. Duan, L. Zhang, Z. Wang, C. Wang and F. Shi, *ACS Appl. Mater. Interfaces*, 2021, **13**, 20681–20688.
51 TaeTTOOz – printable, rechargeable and flexible batteries, https://www.creavis.com/en/success-stories/completed-projects/taettooz, (accessed November 2024).
52 T. P. Nguyen, A. D. Easley, N. Kang, S. Khan, S.-M. Lim, Y. H. Rezenom, S. Wang, D. K. Tran, J. Fan, R. A. Letteri, X. He, L. Su, C.-H. Yu, J. L. Lutkenhaus and K. L. Wooley, *Nature*, 2021, **593**, 61–66.
53 Y. Deng, C. Teng, Y. Wu, K. Zhang and L. Yan, *ChemSusChem*, 2022, **15**, e202102710.
54 U. Ail, J. Phopase, J. Nilsson, Z. U. Khan, O. Inganäs, M. Berggren and X. Crispin, *ACS Sustainable Chem. Eng.*, 2020, **8**, 17933–17944.
55 D. Kumar, U. Ail, Z. Wu, E. M. Björk, M. Berggren, V. Gueskine, X. Crispin and Z. Khan, *Adv. Sustainable Syst.*, 2023, **7**, 2200433.
56 A. Laforgue, C. W. Leung, E. Lam, S. Régnier and R. Black, *Biodegradable Batteries With Redox-Active Polymer Materials*, WO2024/259519, 2024.
57 A. D. Easley, T. Ma and J. L. Lutkenhaus, *Joule*, 2022, **6**, 1743–1749.
58 J. Muñoz-Liesa, M. Navarro-Segarra, M. Sierra-Montoya, J. P. Esquivel and L. Talens Peiró, *Sustain. Prod. Consump.*, 2025, **54**, 202–214.